Simulation of Mixed Layer Depth in the Northeast Pacific Utilizing Spectral Nudging

SHAWN M. DONOHUE AND MICHAEL W. STACEY

Department of Physics, Royal Military College of Canada, Kingston, Ontario, Canada

(Manuscript received 11 May 2010, in final form 1 September 2010)

ABSTRACT

A numerical model, the Parallel Ocean Program (POP), is used to run a 46-yr simulation of the North Pacific Ocean beginning in January 1960. The model has 0.25° horizontal resolution and 28 vertical levels, and it employs spectral nudging, which, unlike standard nudging, nudges only specific frequency and wavenumber bands. This simulation is nudged to the mean and annual Levitus climatological potential temperature and salinity. The model was forced with National Centers for Environmental Prediction (NCEP) mean monthly winds, sea level pressure, net heat flux, and rain rate.

The simulated mixed layer depths (MLD) suggest significant shoaling of the MLD between 1970 and 2006, with faster rates in the northern Gulf of Alaska and slower rates to the west and south of Line Papa. The rates are of similar magnitude to those found in past studies and are consistent with the observed freshening and warming of the upper waters in the Gulf of Alaska. The rates are not spatially uniform, and the simulated MLD in the northeast Pacific actually deepens with time at some locations. These regions of increase form zonal bands in the simulation. The simulated MLD at Ocean Weather Station Papa (OWSP) shoals on average, but it is located close to one of these deepening bands.

On average, the simulated, low-frequency MLD at OWSP gives a good indication of the MLD along Line Papa and in the Gulf of Alaska near Line Papa's latitude. The correlation coefficient between the MLD at OWSP and the latitudinal average of the MLD within the greater Gulf of Alaska (with OWSP removed) is 0.7 at zero lag. The correlation coefficient between the MLD at OWSP and the latitudinal average along Line Papa alone (with OWSP removed) is 0.6 at zero lag. Observed variability of the MLD along Line Papa and at OWSP is reproduced by the model. However, there is considerable spatial variability in the simulated MLD in the Gulf of Alaska as a whole, so MLD variability at OWSP is not necessarily a good indicator of the MLD variability throughout the region. Over the span of the simulation, the low-frequency MLD variability in the Gulf of Alaska is better correlated to the North Pacific Gyre Oscillation (NPGO) than to either the Pacific decadal oscillation (PDO) or Southern Oscillation index (SOI).

1. Introduction

The ocean mixed layer depth (MLD) is one of the most important properties of the upper ocean. Its value parameterizes the depth of the quasi-homogeneous upper layer of the ocean that directly interacts with the atmosphere. The depth of the mixed layer has significant climate, surface acoustic, and biological impacts, as noted by Kara et al. (2000a). The MLD is primarily determined by a balance between the turbulent mixing caused by wind stress and the stratifying buoyancy fluxes of heat and freshwater at the air–sea interface. Broadly speaking, spatial variations in the MLD can be understood by considering the wind stress, the net heat and freshwater fluxes, and the deeper water mass characteristics, which influence the ease with which mixing can penetrate vertically. The MLD is commonly defined as the depth of the sigma-*t* (σ_t) surface, which differs in density by a fixed amount $\Delta\sigma_t$ from that at a reference depth (typically 10 m). For example, Freeland et al. (1997) used $\Delta\sigma_t$ = 0.1 kg m^{-3} to calculate the MLD in the Gulf of Alaska. Other values (e.g., $\Delta\sigma_t$ = 0.125 kg m^{-3}; Kara et al. 2003) have also been used.

Freeland et al. (1997) found that sea surface temperatures (SST) increased and that the sea surface salinity decreased in the northeast Pacific "over the last 60 years." The midwinter MLD was observed to decrease over time in the northeast Pacific. It increased in the subtropical and transition regions and decreased in the northern Gulf of Alaska.

Whitney and Freeland (1999) reviewed oceanographic properties in the vicinity of Ocean Weather Station Papa

Corresponding author address: Shawn M. Donohue, Department of Physics, Royal Military College of Canada, P.O. Box 17000 STN Forces, Kingston ON K7K 7B4, Canada.
E-mail: shawn.donohue@rmc.ca

DOI: 10.1175/2010JPO4499.1

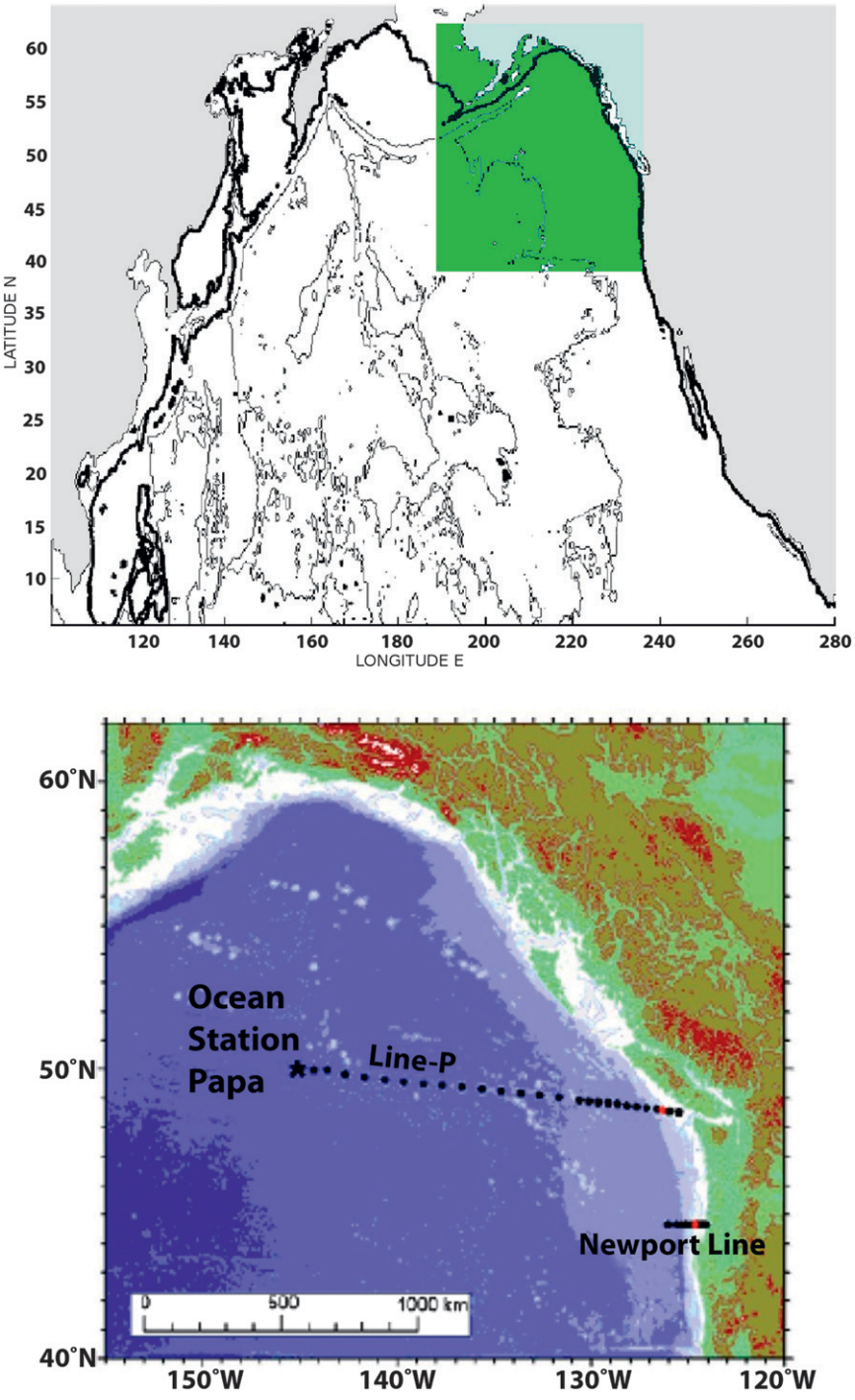

FIG. 1. (top) The model domain consists of 741 × 319 horizontal grid points. The northeast Pacific (the green region) is our primary region of interest. OWSP is located at 50°N, 215°E (145°W). The bathymetry is from Smith and Sandwell (1997). (bottom) Shown is Line Papa (DFO 2004), where each dot represents a sampling location.

(OWSP) with data collected over 42 yr. They reported rates of change for T, S, and σ_t at the surface of 1.2°C, −0.2 psu, and −0.3 kg m^{-3} per century, respectively, with all significant at the 95% level.

Cummins and Lagerloef (2002) used National Centers for Environmental Prediction (NCEP) winds with a simple one-dimensional, stochastic model to simulate the influence of Ekman pumping on the pycnocline depth (a proxy for MLD) over the period 1948–2000 at OWSP. The pycnocline was deeper than the long-term average before the late 1970s and shallower after, in agreement with the finding of Freeland et al. (1997) that the MLD has tended to shoal.

Li et al. (2005) performed the first detailed historical study of the MLD variability along the entire Line Papa, focusing on both long-term and seasonal variability. Their analysis of over 46 yr of observations (broken into pre- and post-1976 segments) along the original 13 stations of Line Papa shows that, after 1976, the February offshore (coastal) MLD was less (more) than before 1976. They also found however that the largest winter MLD shifted from being in February before 1976 to being in April after 1976 and that if the pre-1976 February average MLD (49.9 m) was compared to the post-1976 April average MLD (52.1 m) then there was not much of a change.

Capotondi et al. (2005) extended the Cummins and Lagerloef (2002) study by using an ocean general circulation model. Their results show the pycnocline deepening as a broad coastal band and shoaling in the central Gulf of Alaska after 1977, primarily because of changes in Ekman pumping. Their model supports the shoaling of the MLD in the late fall (December onward) through February, in agreement with Freeland et al. (1997).

Jackson et al. (2009) simulated MLD using a simple one-dimensional model for the period 2001–05 and found that the MLD at OWSP behaved differently than at other stations in the Gulf of Alaska. They suggest OWSP's location may not be a true proxy indicator of the state of the MLD for the entire Gulf of Alaska.

This study is the first to apply spectral nudging filter in a model to simulate the evolution of the MLD in the Pacific Ocean with particular emphasis along Line Papa and the northeast Pacific. The simulation will be shown to successfully reproduce much of the variability of the MLD.

This paper is organized as follows: Section 2 will briefly discuss the model and spectral nudging. Section 3 will outline the results, and section 4 is the discussion and conclusions.

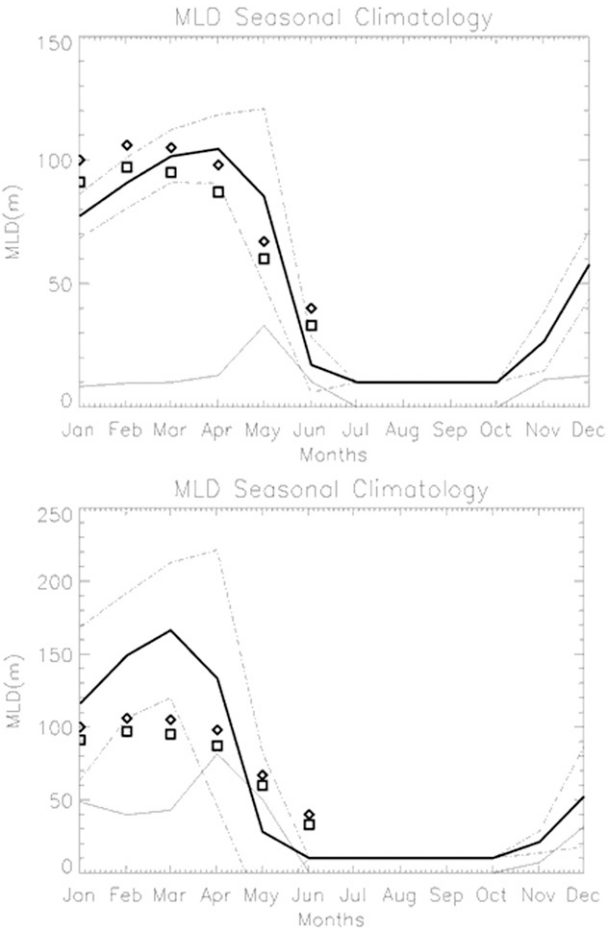

FIG. 2. The monthly climatology for the (top) nudged and (bottom) nonnudged simulations (thick solid line), averaged over 1980–2006. The dashed lines are the 75% confidence intervals for the MLDs. The thin solid lines are the monthly standard deviations. Note that the top and bottom panels have different vertical scales. The icons are from the NRL (available online at http://www7320.nrlssc.navy.mil/nmld/nmld.html; squares) and Li et al. (2005; diamonds) climatology at OWSP.

2. Model

A detailed description of the Parallel Ocean Program (POP) can be found in Maltrud et al. (1998) and Smith et al. (2000), and details about the spectral nudging technique can be found in Thompson et al. (2006) and Wright et al. (2006). The model setup for the North Pacific simulation discussed in this paper is the same as that used by Stacey et al. (2006) and Shore et al. (2008), with three major exceptions: 1) they used climatological forcing, whereas this study has used the mean monthly NCEP observations/reanalyses; 2) the model used here is nudged to the Levitus monthly climatology only, without melding additional climatology obtained from the Institute of Ocean Sciences (IOS); and 3) the model used here has 28 vertical levels (Table 1). The model domain is shown in Fig. 1. It includes essentially the entire North Pacific.

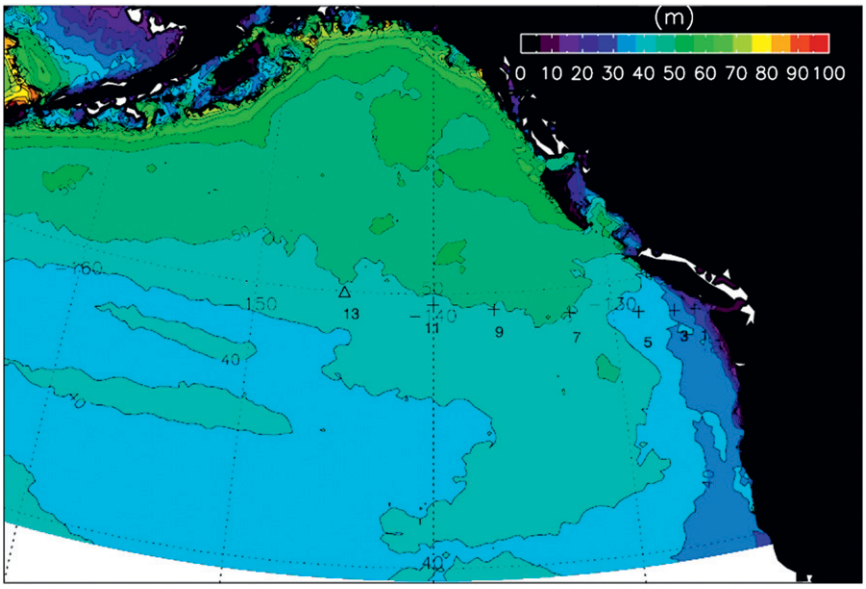

FIG. 3. The simulated, 36-yr average MLD contour map. The numbered crosses indicate odd numbered Line Papa stations. The open triangle (number 13) indicates the location of OWSP.

The model was spectrally nudged toward the mean and annual potential temperature (θ) and salinity (S) Levitus climatologies with a restoring time scale of 20 days. The monthly climatological observations were also required for the sponge layer at the southern boundary and for the determination of surface heat and freshwater fluxes. The latter included observed flux estimates plus restoring toward monthly climatological sea surface values of θ and S with a relaxation time scale of 50 days.

The model used the K-profile parameterization (KPP) vertical mixing scheme as outlined in Large et al. (1994). Large et al. have shown KPP to be accurate in the North Pacific, particularly at OWSP, for estimating thermocline depths and MLDs.

The model was spun up from rest, beginning on 1 January 1960, and run for 46 yr of simulation time. The first 10 yr of the simulation (1960–70) was considered to be spinup time.

3. Results

The usefulness of the spectral nudging technique for calculating MLD was first investigated. Figure 2 shows the climatological MLDs at OWSP using POP, both with and without spectral nudging. Also shown are the monthly standard deviations and the 75% confidence intervals. The simulated climatological monthly MLD at OWSP for winter through spring from the Naval Research Laboratory (NRL; squares) and from observations (Li et al. 2005; diamonds) are also shown. In Fig. 2, the simple definition of MLD has been used for the simulation with $\Delta\sigma_t = 0.1$ kg m^{-3}, except during the summer, when the MLD is given the value of 10 m. (We are interested in the nonsummertime MLDs and will concentrate on those in this paper; also, when necessary, linear interpolation between grid points has been used in calculating the MLD.) One can easily see that, when spectral nudging is used, the MLD profile agrees well with the NRL estimate and with the observations, whereas, when it is not used, the MLD is significantly overestimated and much less constrained. Note also that when spectral nudging is used, the standard deviation is maximized in the spring, in agreement with observations (Li et al. 2005).

The obvious necessity to use spectral nudging to get a reasonable MLD shows that the model without nudging is clearly inadequate. One reason for this inadequacy is numerical diffusion caused by the relatively coarse spatial resolution that is being used, but another reason may be that the monthly winds do not have enough temporal resolution to include processes that can significantly affect the MLD over shorter than monthly time scales (e.g., single intense storms, frontogenesis). Spectral nudging could therefore be nudging the model toward a realistic simulation of the MLD for reasons not solely related to the spatial resolution being used here.

Another method of estimating the MLD was tried, Estimating the Circulation and Climate of the Ocean (ECCO; e.g. Lorbacher et al. 2006), and it was found to produce MLDs consistent with those produced using the simpler method used here. Li et al. (2005), whose results will be compared to the simulation, used the method of Kara et al. (2000b) to estimate the MLD, and their

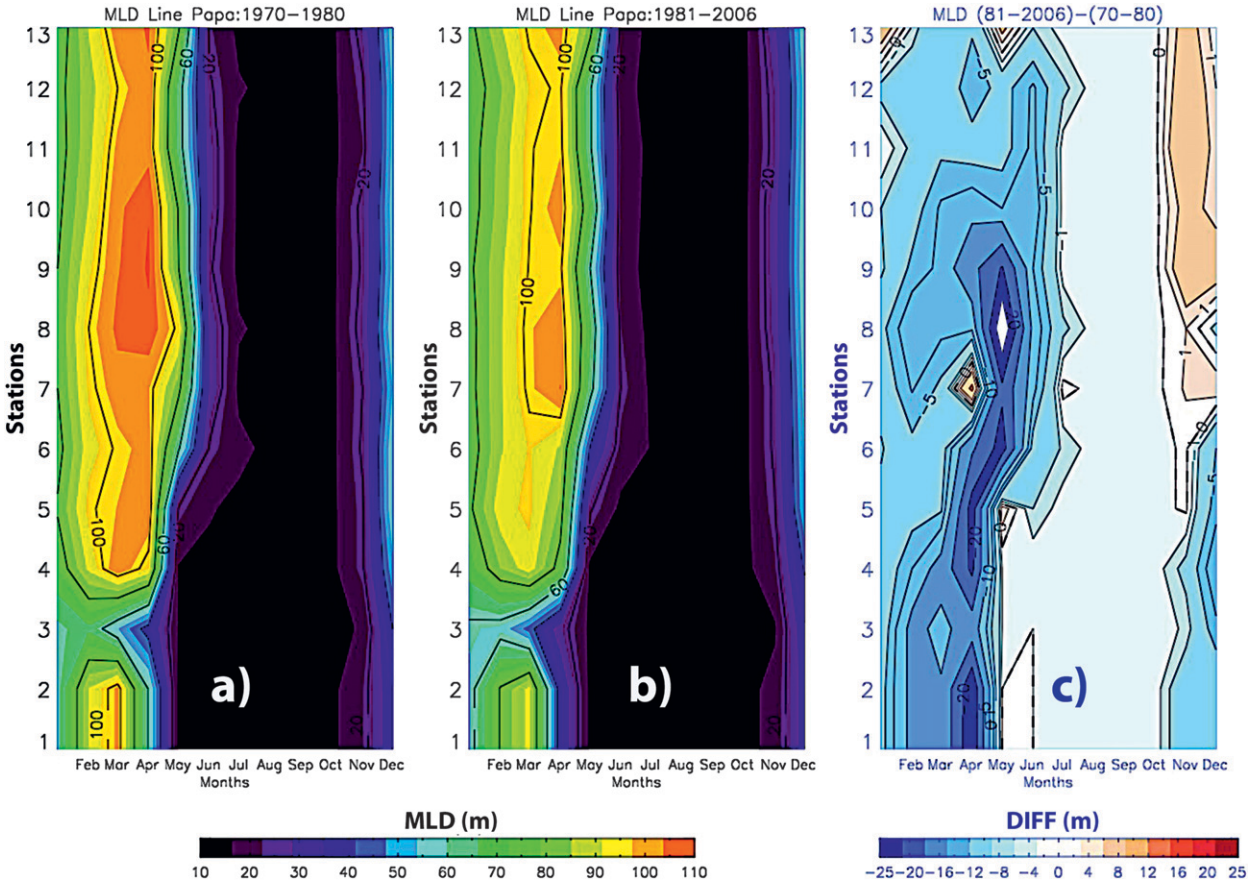

FIG. 4. Monthly MLD values along Line Papa, averaged for each month of the year over two time frames: (a) 1970–80 and (b) 1981–2006. (c) A difference plot of MLD at 1981–2006 minus MLD at 1970–80 is shown.

results (Fig. 2 and see below) are consistent with the simpler method also.

Figure 3 shows the MLD averaged over the entire length of the simulation. The average value is less than 80 m essentially everywhere. When the average MLD at OWSP is calculated over two time intervals, 1970–80 and 1981–2006, one obtains 49 and 51 m, respectively. (The values are slightly larger when the summertime MLD is set to 20 m.) Li et al. (2005), using the time intervals 1957–76 and 1977–96, calculated 49.9 and 52.1 m, respectively, for the MLD at OWSP. They chose these time intervals to look for changes in the MLD caused by the 1976/77 regime shift and concluded that there was not a significant change.

Figures 4a,b shows the average simulated MLD along Line Papa for the time intervals 1970–80 and 1981–2006. (The summertime MLD values, set to 10 m, are obviously of no physical significance; also, values closer to shore than about station 3 should be treated with caution.) Note that away from the coast the MLD tends to be less during the latter time period, in broad agreement with the observed tendency of the wintertime MLD to shoal over time (Freeland et al. 1997; Li et al. 2005). Between December and April/May, according to the model, the offshore MLD decreased by about 5–10 m.

Figure 5 shows bar plots, averaged over 25 yr, of the MLD at nine stations (5–13) for the later time period (1981–2006), and it is clear the MLD undergoes a marked decrease in April–June and deepens in the autumn in November and December. Close to shore the decrease occurs in April and May and farther from shore it occurs in May and June, in agreement with the observation (Li et al. 2005) that the transition occurs at a later time farther offshore. Note also that the maximum MLD occurs in April, in agreement with the results of Li et al. (2005). At times earlier than 1980 in the simulation, the maximum MLD shifts to earlier months, in agreement with Li et al. (2005), although a direct comparison is difficult because the simulation begins at a time later than the observations used by Li et al. (2005) and the model's initial 10 yr of simulation is considered spinup.

Figure 6 shows pentads of the MLD anomalies at OWSP. Both the simulated values and the values calculated from observations (Li et al. 2005) are shown. One

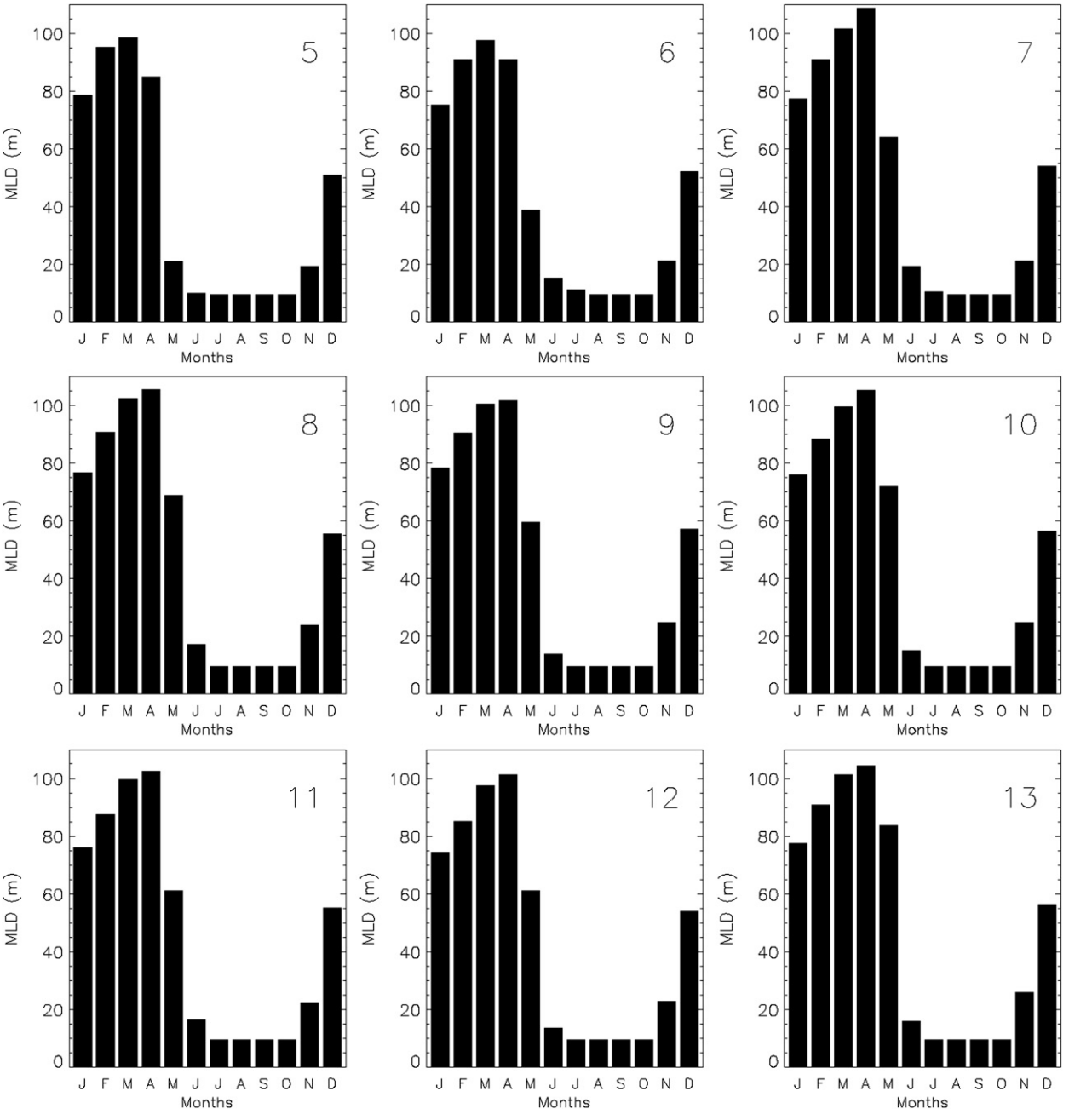

FIG. 5. The monthly MLDs at stations 5–13 (OWSP), averaged over 1981–2006.

sees that there is good agreement between the simulated values and the values calculated from the observations. There is only a simulated value for the large negative anomaly in 2001–06, but it is known that the MLD shoaled significantly during that time (H. Freeland 2007, personal communication). The correlation coefficient between observations and model is 0.8 at zero lag. The ratio of the sum of the square of the residuals between the model and the observations to the variance in the observations is 0.3.

Figure 7a shows a contour plot of the simulated MLD anomalies at 50°N (the MLDs were low-pass filtered to remove the annual cycle), over a wide range of longitudes in the northeast Pacific from 1970 to 2006 (OWSP is located at 215°E). Figure 7b shows the time series of the MLD anomalies at OWSP (solid line) and also the time series of the longitudinally averaged (using the values in Fig. 7a but with OWSP's contribution removed) MLD anomalies. The correlation coefficient at

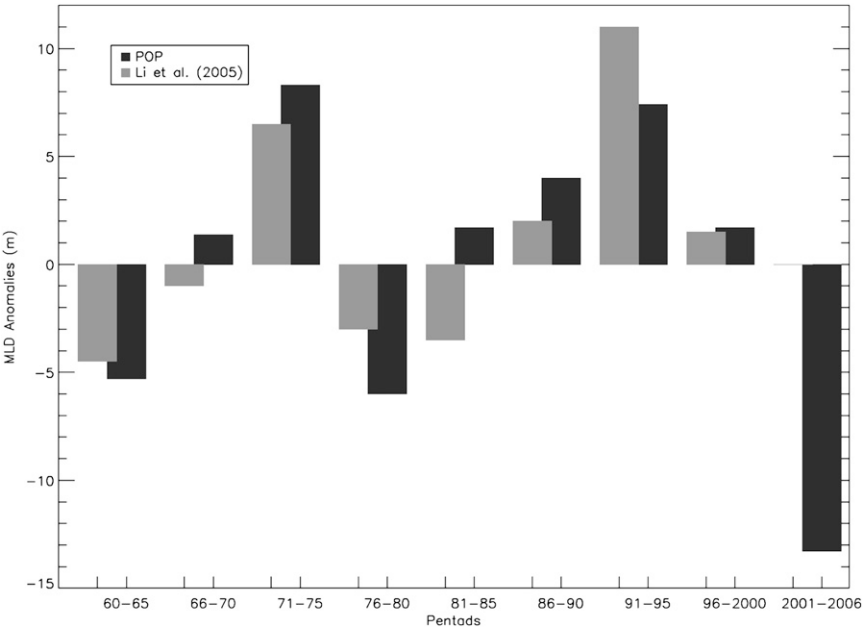

FIG. 6. Pentads of the simulated MLDs and also MLDs calculated from values reported in Li et al. (2005) detailed pentad observations at OWSP. These pentads shown here have been calculated using both winter (December–February) and spring (March–May) values. Li et al. report the winter and spring values separately and did not give a value for 2001–06. The correlation is 0.8. The ratio of the sum of the square of the residuals to the variance in the observations is 0.3. The variances are 24.5 m^2 (model) and 25.7 m^2 (observations).

zero lag between the two time series is 0.7, showing that the MLD at OWSP is indicative of MLD at 50°N over a broad range of longitudes.

Figure 8 is a contour map of the correlation coefficient (at zero lag) between the MLD anomalies in the Gulf of Alaska and the MLD anomalies at OWSP. The contours show that the MLD anomalies at OWSP tend to be more representative of the anomalies along zonal bands than of the anomalies in the meridional direction. Overall, the MLD at OWSP has a 0.6 or greater correlation with a significant portion of the MLDs in the Gulf of Alaska. The MLD variance over the entire area has an average of 10 m^2, whereas the variance at OWSP is 15 m^2, so the magnitude of the variability is greater at OWSP than over the Gulf of Alaska as a whole. Regardless, although there is considerable variability in the simulated MLD anomalies over the northeast Pacific, these correlations suggest that the MLD at OWSP is a proxy for the MLDs elsewhere as well and therefore that its variability may be caused to a significant extent by large-scale influences in the northeast Pacific.

Figure 9 shows the first two EOF modes of the simulated MLD in the northeast Pacific. Mode 1 (2) explains 29% (13%) of the variance [mode 3 (not shown) explains 8% of the variance]. The annual and shorter periods were removed before calculating these EOFs. Mode 1 (Fig. 9a) tends to increase and decrease in phase over the entire northeast Pacific, decaying in amplitude toward the west with peak values along the coast, whereas mode 2 (Fig. 9b) tends to increase on one side of a roughly north–south line while decreasing on the other side and vice versa. OWSP is quite close to this line. Also, note that there is some zonal banding in mode 1, suggestive of the influence of two-dimensional turbulence (e.g., Maximenko et al. 2008). This influence may explain in part the pattern of the correlation contours in Fig. 8.

The time series (Fig. 9c), when compared to the MLD anomalies in Fig. 6 (and taking into account the sign of their spatial structure; Figs. 9a,b), show that both mode 1 and 2 constructively interfered to influence the large negative anomaly at OWSP in 2001–06. The positive anomaly in 1991–95 was influenced primarily by mode 2. The positive anomaly in 1971–75 was influenced primarily by mode 1, counteracting the influence of mode 2. This can be seen more clearly in Fig. 9d, where the time series have been averaged over 5 yr and their relative magnitudes scaled by the following ratio: mode 1/mode 2 $\sim$ 29/13.

Note that the influence of mode 2 on the MLD at OWSP (see Fig. 9b) is similar to its influence on the MLD to the south and west of OWSP but that its influence to the north and east of OWSP is out of phase with its influence at OWSP. This property of mode 2 is

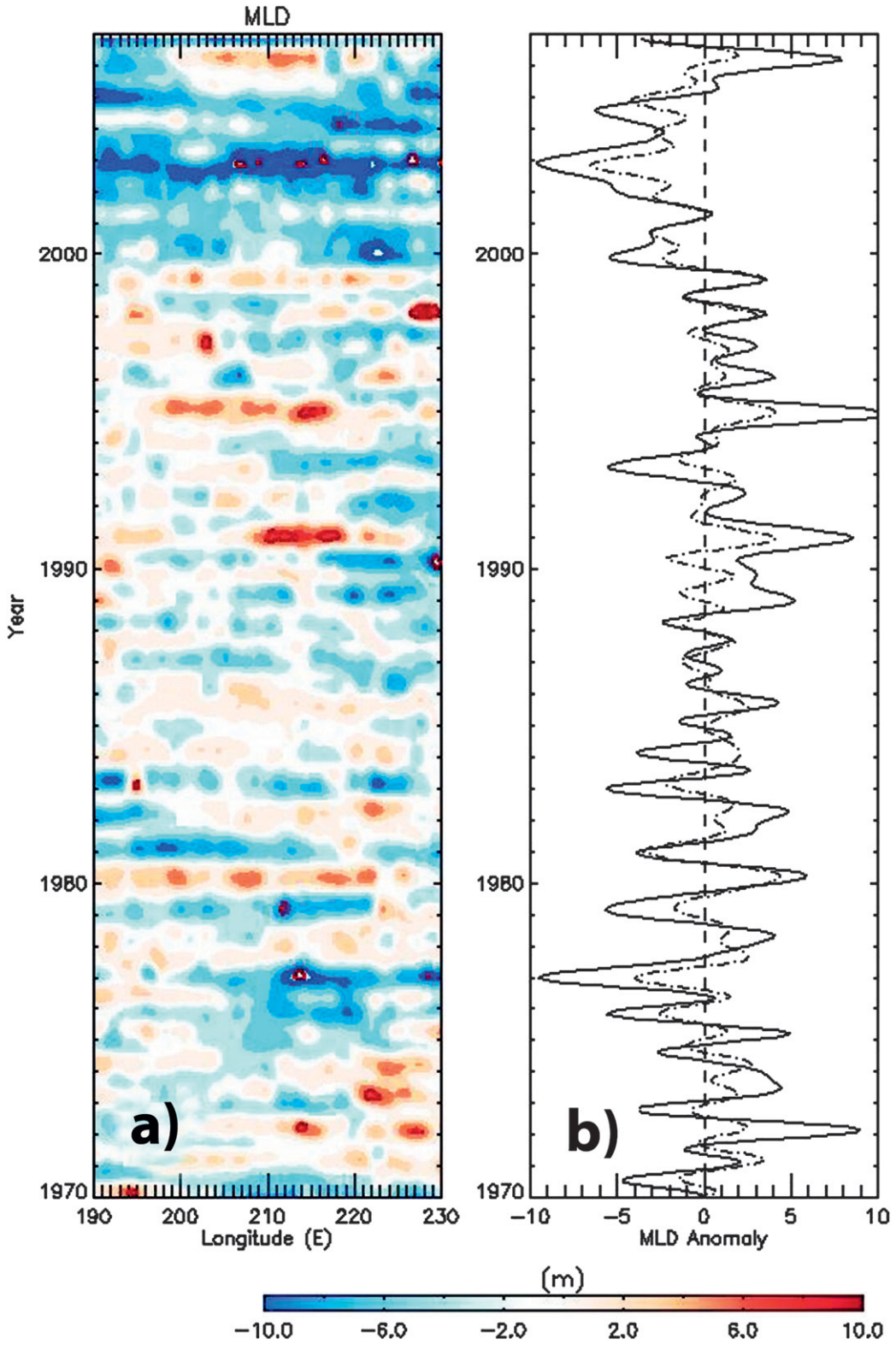

FIG. 7. (a) The simulated, MLD anomalies at 50°N. (The annual and shorter periods have been removed.) OWSP's longitude is found at 215°E. (b) The dashed line is the longitudinally averaged MLD anomalies using the values on the left, and the solid line uses the values from OWSP only.

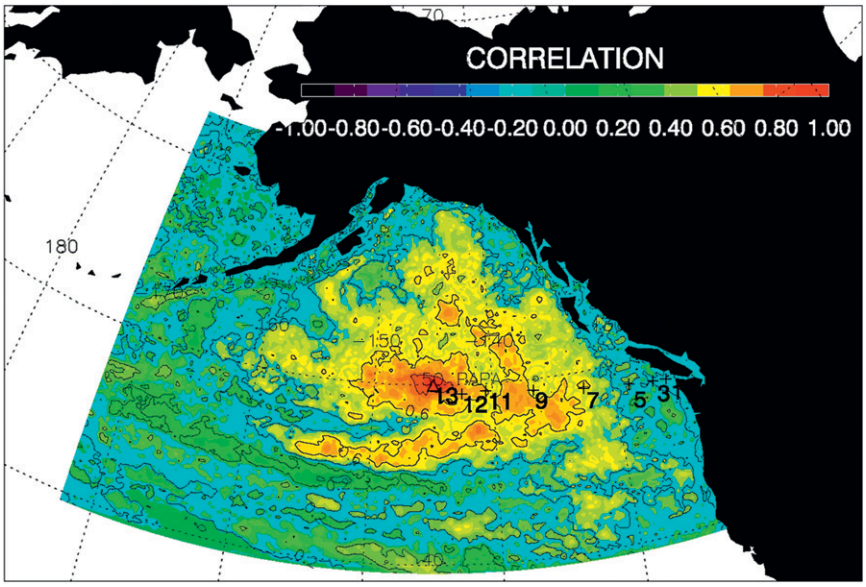

FIG. 8. The correlation coefficient between the MLD anomaly at OWSP (station 13; open, black triangle) and the MLDs at other locations in the Gulf of Alaska. Contours represent the Pearson coefficients.

consistent with the suggestion of Jackson et al. (2009) that what happens at OWSP may be consistent with what happens to the south of OWSP but may not be consistent with changes to the north and east.

Mode 2 is correlated to three major indexes, the Southern Oscillation index (SOI), Pacific decadal oscillation (PDO), and North Pacific Gyre Oscillation (NPGO; Di Lorenzo et al. 2008). But mode 1 is correlated only to the NPGO (Table 2). (At a period of 5 yr, the coherence between the NPGO and mode 1 is about 0.8, and they are about 180° out of phase.) Because mode 1 has more than twice the energy as mode 2, this suggests that the NPGO has more influence on the MLD than the PDO or SOI do. This correlation with the NPGO supports the suggestion made earlier that MLD variability in the northeast Pacific may be caused in part by large-scale influences.

Figure 10a shows the mode-1 time series of the simulated MLD plotted over the time series of the inverted NPGO index. (By ''inverted'' we mean that the NPGO index has been multiplied by -1 to account for the almost 180° phase difference and therefore to make a visual comparison easier.) Comparing the NPGO index time series to the MLDs at OWSP (Fig. 6), one sees that a positive NPGO index is associated with negative MLD anomalies at OWSP during 1976–80 and 2001–06. Also, a negative NPGO index is associated with a positive MLD anomaly during 1991–95. Interestingly, the positive MLD in 1971–75 does not appear to be associated with the NPGO, and the relatively high NPGO index in the late 1980s does not appear to be related to an extremum in the MLD at OWSP.

Figure 10b shows the time series of the mode-1 EOF of the stratification plotted over the time series of the inverted NPGO index. Stratification as defined here is the σ_t difference between the surface and 75 m. This is the same definition as that commonly used by H. Freeland (2008, personal communication). The maximum correlation coefficient between the two time series (i.e., the stratification and the ''noninverted'' NPGO index) is -0.6 with the NPGO index (not inverted) leading by about six months. As shown in Fig. 10b, a positive mode-1 value corresponds to a decrease in stratification. One sees that a negative inverted NPGO index (i.e., a positive NPGO index) tends to correspond to negative MLD anomalies and to increases in stratification. Note in particular that the three biggest positive values of the NPGO index correspond to increases in stratification. The large positive phase of the NPGO index corresponded to strong negative salinity anomalies in the model with anomaly cores between 100- and 150-m depth. These three positive NPGO index phases were further found to correspond to three significant increases (decreases) in the upper layer (top 100 m) mode-1 EOFs of the temperature (density) anomalies (not shown). There was a corresponding increase in the upper-layer stratification. This increase was found to be stronger offshore along Line Papa toward the center of the Gulf of Alaska.

Figure 11 shows the simulated MLD anomalies at OWSP (solid line; also see Fig. 7b) and a time series of

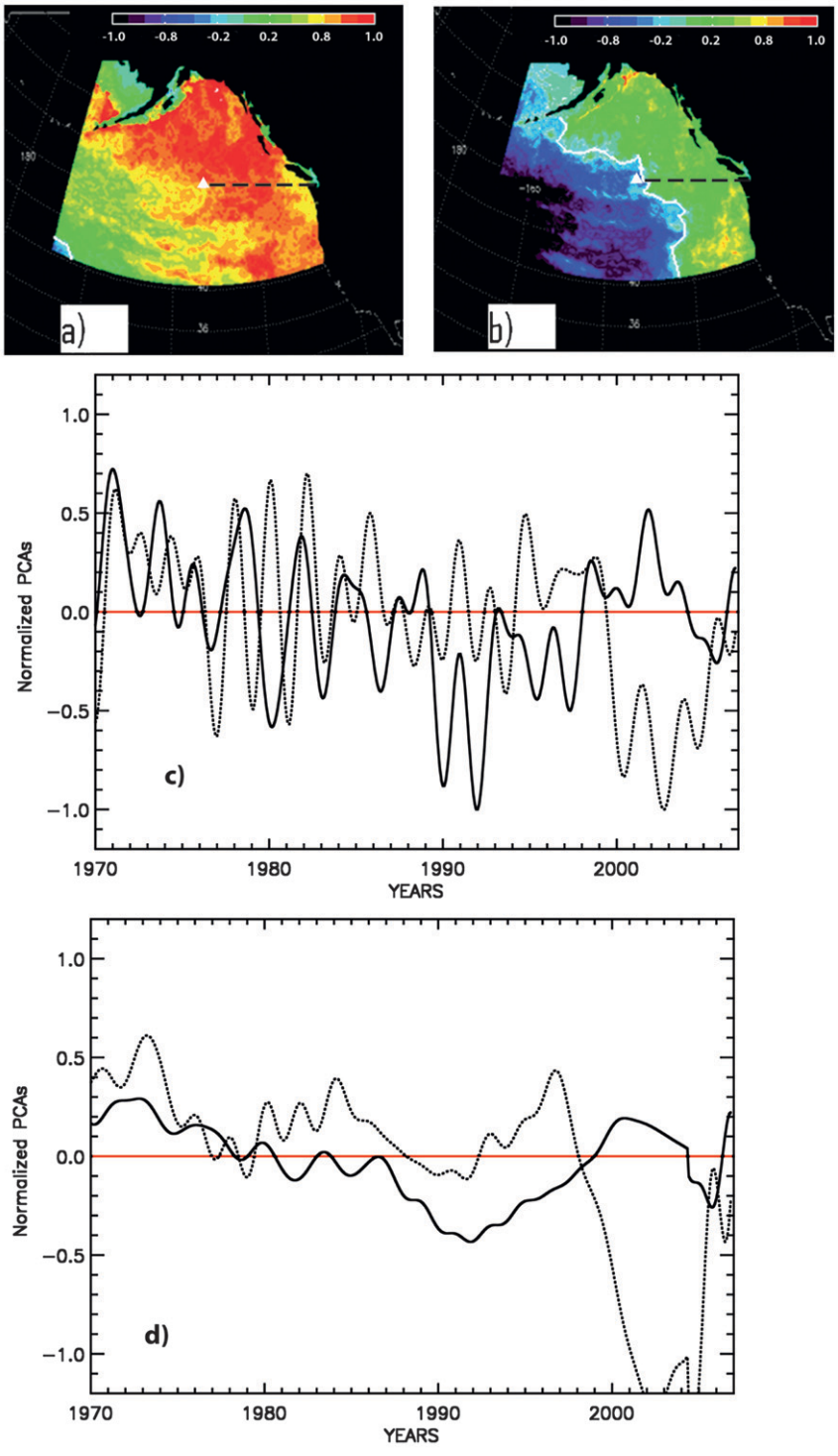

FIG. 9. The first two EOF modes of the MLD anomalies in the northeast Pacific. The annual and shorter periods were removed before calculating the EOFs. Shown are the spatial dependences of modes (a) 1 and (b) 2. Mode 1 (2) explains 29% (13%) of the variance. Mode 3, not shown, explains 8% of the variance. The solid white lines are the zero contours. The dashed black line is Line Papa. (c) The (normalized) time dependence (principal components) of the two modes; the dotted (solid) line is for mode 1 (2). (c),(d) The time dependences of the modes, but the values in (c),(d) have been averaged over 5 yr and adjusted to reflect the variances each mode explains. The solid white triangle in (a),(b) indicates the location of OWSP.

TABLE 1. Layer thicknesses for the model. The top and bottom of each layer is a vertical velocity (w) point. Midway between each layer and below the w point is a potential temperature, salinity, and pressure (θ, S, p) point; midway between each layer and offset is a horizontal velocity point. Stacey et al. (2006) and Shore et al. (2008) used 23 vertical levels.

No.	Layer thickness (m)	No.	Layer thickness (m)
1	10	15	10
2	10	16	25
3	10	17	50
4	10	18	100
5	10	19	200
6	10	20	500
7	10	21	500
8	10	22	500
9	10	23	500
10	10	24	500
11	10	25	500
12	10	26	500
13	10	27	500
14	10	28	500

TABLE 2. The maximum correlation coefficients between modes 1 and 2 and the SOI, PDO, and NPGO. If there is no correlation coefficient that is significantly nonzero, then no value is given. This lack of correlation occurs between mode 1 and the SOI and PDO. The values in parentheses indicate the time lag that maximizes the correlation. A positive value indicates that the indices lead the mode.

	SOI	PDO	NPGO
Mode 1	—	—	−0.5 (1 yr)
Mode 2	0.4 (0, 2.5 yr)	−0.5 (0, 2 yr)	0.4 (0 yr)

the MLD at OWSP (dashed line) constructed solely from the two EOFs shown in Fig. 9. The correlation coefficient between the two time series is 0.5 at zero lag. The variance of the time series constructed from the first two EOFs is about 12 m^2, which is quite close to the actual simulated MLD variance at OWSP of 15 m^2. (Regionwide, the first two EOFs explain only 42% of the variance.) This result suggests that the first two EOFs explain much more of the MLD variability at OWSP than they do of the variability regionwide.

Figure 12 shows the simulated time rate of change in the winter MLD, time averaged from 1970 to 2006. The simulated time rate of change at OWSP is −20 m per century with an uncertainty of 10 m, and the value estimated from observations by Freeland et al. (1997) is −60 m per century with an uncertainty of 20 m per century. According to the simulation, the MLD is shoaling over much of the North Pacific, but there are significant (banded) regions where deepening is occurring. OWSP is located near one of these bands, suggesting that what happens there may be quite sensitive to small changes in forcing. Jackson et al. (2009) have suggested that what happens at OWSP may not be indicative of the northeast Pacific as a whole, and this simulation supports that view. According to the

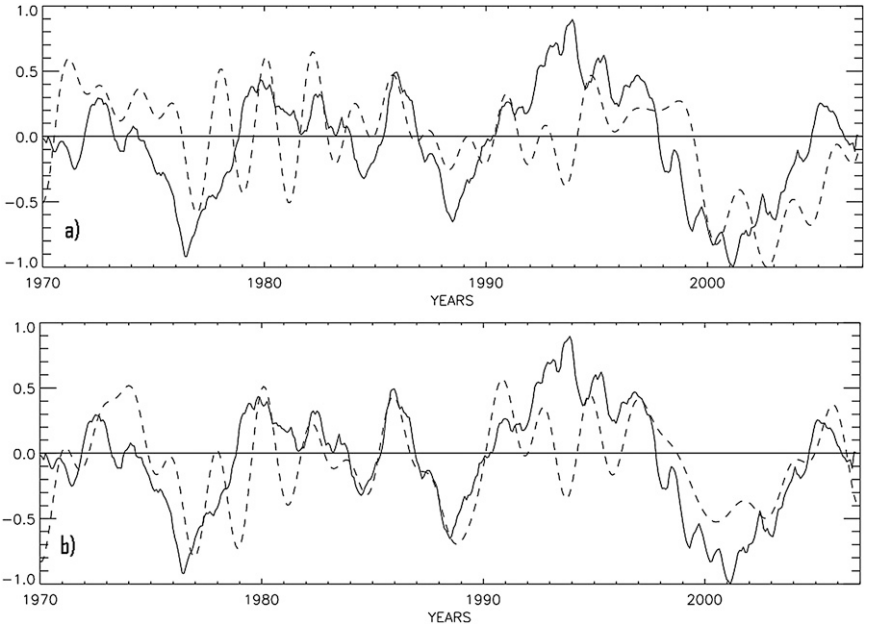

FIG. 10. (a) The normalized inverted NPGO index (solid line) and the mode-1, low-passed MLD time series (dashed line). (b) As in (a), but with the mode-1, low-passed stratification time series. Negative values of the MLD (stratification) indicate shoaling (increased stratification).

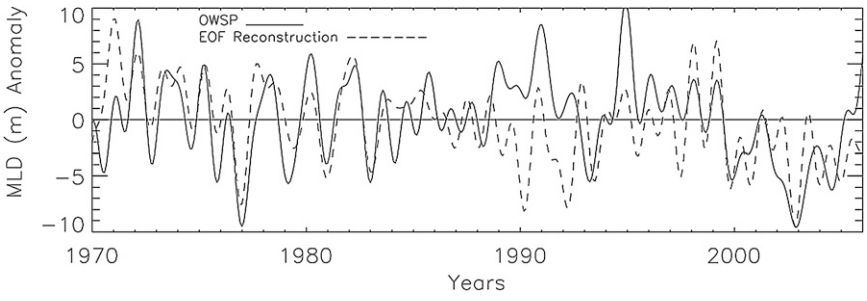

FIG. 11. The simulated MLD anomalies at OWSP (solid line; also shown in Fig. 7b) and the MLD anomalies at OWSP constructed from the two EOFs shown in Fig. 9.

simulation, what happens at OWSP can be indicative of what is happening on average over rather large portions of the northeast Pacific, but over the entire expanse of the northeast Pacific there is considerable variability. The banded regions correspond to locations where there is deepening over time and may, as suggested for the bands present in the mode-1 MLD EOF, be related to two-dimensional turbulence.

4. Discussion and conclusions

A numerical model that uses spectral nudging has been shown to reproduce MLD values calculated from observations at OWSP. The model has 0.25° horizontal resolution and 10-m vertical resolution near the surface. When spectral nudging is not used in the model, the simulation yields MLDs that are completely unrealistic. The simulated MLDs at OWSP and along Line Papa were compared are those given by Li et al. (2005).

In agreement with observations, the variance in the MLD is greatest in the spring, and the spring/summer decrease in MLD from winter values occurs later as one moves offshore. There is an appearance of early shoaling in the late fall, particularly December onward, as observed along Line Papa.

According to the simulation, the MLD anomalies at OWSP are indicative of what happens along Line Papa as a whole (0.6 correlation at zero lag) and the greater

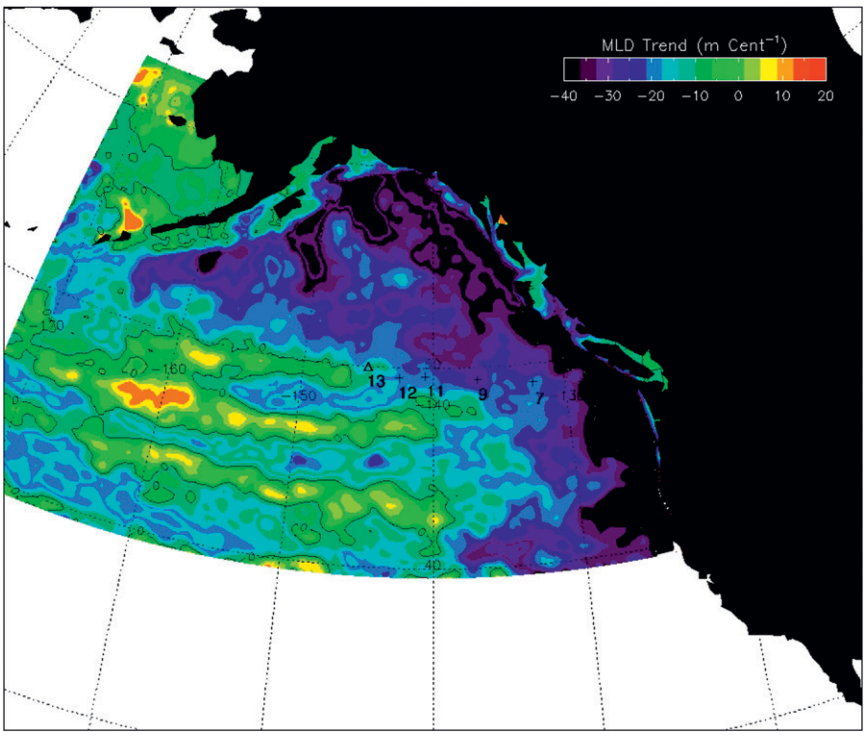

FIG. 12. Contour map of the MLD trends (in meters per century) in the northeast Pacific, using January–April values from 1970 to 2006. OWSP is indicated by the numeral 13.

Gulf of Alaska at the same latitude (0.7 correlation at zero lag), and therefore the anomalies there may be influenced by spatially large-scale events. The MLD at OWSP is significantly correlated with a significant portion of the MLDs throughout the Gulf of Alaska.

However, there is considerable variability over the northeast Pacific as a whole, and therefore what happens at OWSP cannot be taken as a proxy for what happens over the entire northeast Pacific. The NPGO has, according to the simulation, more influence on the MLD anomalies than either the SOI or the PDO (Table 2).

Over the course of the simulation, the MLD at OWSP decreases with time on average, as it does over much of the northeast Pacific. Observations (e.g., Freeland et al. 1997; Royer and Grosch 2006) also indicate that the MLD decreases at OWSP. However, the simulation also predicts that there are significant regions of the northeast Pacific where the MLD increases. These regions of increase tend to occur in zonal bands and correspond to regions where banding may occur because of Rossby waves and two-dimensional turbulence. Whether these regions of MLD increase are real in the sense that they would manifest themselves over even longer time averages than the 36 yr of this simulation or are transient effects that would average out over longer time periods waits to be seen.

Acknowledgments. This research has been supported by grants from the Canadian Foundation for Climate and Atmospheric Research (CFCAS). The simulations were run at the High Performance Computing Virtual Laboratory (HPCVL). We thank Howard Freeland for providing us with his refined values for MLD and Argo observations. We thank two reviewers for their kind comments and suggestions.

REFERENCES

Capotondi, A., M. Alexander, C. Deser, and A. J. Miller, 2005: Low-frequency pycnocline variability in the northeast Pacific. *J. Phys. Oceanogr.,* **35,** 1403–1420.

Cummins, P., and G. S. E. Lagerloef, 2002: Low-frequency pycnocline depth variability at Ocean Weather Station P in the northeast Pacific. *J. Phys. Oceanogr.,* **32,** 3207–3215.

DFO 2004: 2003 Pacific region state of the ocean. DFO Science Ocean Status Rep. 2003.

Di Lorenzo, E., and Coauthors, 2008: North Pacific Gyre Oscillation links ocean climate and ecosystem change. *Geophys. Res. Lett.,* **35,** L08607, doi:10.1029/2007GL032838.

Freeland, H., K. Denman, C. Wong, F. Whitney, and R. Jacques, 1997: Evidence of change in the winter mixed layer depth in the northeast Pacific Ocean. *Deep-Sea Res. I,* **44,** 2117–2129.

Jackson, J. M., P. G. Myers, and D. Ianson, 2009: An examination of the mixed layer sensitivity in the northeast Pacific Ocean from July 2001-July 2005 using the General Ocean Turbulent Model and Argo data. *Atmos.–Ocean,* **47,** 139–153, doi:10.3137/OC308.2009.

Kara, A. B., P. A. Rochford, and H. E. Hurlburt, 2000a: Mixed layer depth variability and barrier layer formation over the North Pacific Ocean. *J. Geophys. Res.,* **105** (C7), 16 783–16 801.

——, ——, and ——, 2000b: An optimal definition for ocean mixed layer depth. *J. Geophys. Res.,* **105** (C7), 16 803–16 821.

——, ——, and ——, 2003: Mixed layer depth variability over the global ocean. *J. Geophys. Res.,* **108,** 3079, doi:10.1029/2000JC000736.

Large, W., J. McWilliams, and S. Doney, 1994: Oceanic vertical mixing: A review and a model with a nonlocal boundary layer parameterization. *Rev. Geophys.,* **32,** 363–403.

Li, M., P. G. Myers, and H. Freeland, 2005: An examination of historical mixed layer depths along Line P in the Gulf of Alaska. *Geophys. Res. Lett.,* **32,** L0613, doi:10.1029/2004GL021911.

Lorbacher, K., D. Dommenget, P. P. Niiler, and A. Köhl, 2006: Ocean mixed layer depth: A subsurface proxy of ocean-atmosphere variability. *J. Geophys. Res.,* **111,** C07010, doi:10.1029/2003JC002157.

Maltrud, M. E., R. D. Smith, A. J. Semtner, and R. C. Malone, 1998: Global eddy-resolving ocean simulations driven by 1985–1995 atmospheric winds. *J. Geophys. Res.,* **103,** 30 825–30 853.

Maximenko, N. A., O. V. Melnichenco, P. P. Niiler, and H. Sasaki, 2008: Stationary mesoscale jet-like features in the ocean. *Geophys. Res. Lett.,* **35,** L08603, doi:10.1029/2008GL033267.

Royer, T. C., and C. E. Grosch, 2006: Ocean warming and freshening in the northern Gulf of Alaska. *Geophys. Res. Lett.,* **33,** L166505, doi:10.1029/2006GL026767.

Shore, J., M. W. Stacey, and D. G. Wright, 2008: Sources of eddy energy simulated by a model of the northeast Pacific Ocean. *J. Phys. Oceanogr.,* **38,** 2283–2293, doi:10.1175/2008JPO3800.1.

Smith, R. D., M. E. Maltrud, F. O. Bryan, and M. W. Hecht, 2000: Numerical simulation of the North Atlantic Ocean at 1/10°. *J. Phys. Oceanogr.,* **30,** 1532–1561.

Smith, W. H. F., and D. T. Sandwell, 1997: Global sea floor topography from satellite altimetry and ship depth soundings. *Science,* **277,** 1956–1961.

Stacey, M. W., J. Shore, D. G. Wright, and K. R. Thompson, 2006: Modeling events of sea-surface variability using spectral nudging in an eddy permitting model of the northeast Pacific Ocean. *J. Geophys. Res.,* **111,** C06037, doi:10.1029/2005JC003278.

Thompson, K. R., D. G. Wright, Y. Lu, and E. Demirov, 2006: A simple method for reducing seasonal bias and drift in eddy resolving ocean models. *Ocean Modell.,* **13,** 109–125.

Whitney, F., and H. Freeland, 1999: Variability in upper-ocean water properties in the NE Pacific Ocean. *Deep-Sea Res. II,* **46,** 2351–2370.

Wright, D. G., K. R. Thompson, and Y. Lu, 2006: Assimilating long-term hydrographic information into an eddy-permitting model of the North Atlantic. *J. Geophys. Res.,* **111,** C09022, doi:10.1029/2005JC003200.